We are IntechOpen, the world's leading publisher of Open Access books Built by scientists, for scientists

6,900
Open access books available

185,000
International authors and editors

200M
Downloads

Our authors are among the

154
Countries delivered to

TOP 1%
most cited scientists

12.2%
Contributors from top 500 universities



WEB OF SCIENCE™

Selection of our books indexed in the Book Citation Index in Web of Science™ Core Collection (BKCI)

Interested in publishing with us?
Contact book.department@intechopen.com

Numbers displayed above are based on latest data collected.
For more information visit www.intechopen.com



Chapter

Microgrid System Reliability

Razzaqul Ahshan

Abstract

This chapter presents the reliability evaluation of a microgrid system considering the intermittency effect of renewable energy sources such as wind. One of the main objectives of constructing a microgrid system is to ensure reliable power supply to loads in the microgrid. Therefore, it is essential to evaluate the reliability of power generation of the microgrid under various uncertainties. This is due to the stochastically varying wind speed and change in microgrid operational modes which are the major factors to influence the generating capacity of the individual generating unit in the microgrid. Reliability models of various subsystems of a 3-MW wind generation system are developed. The impact of stochastically varying wind speed to generate power by the wind turbine system is accounted in developing sub-system reliability model. A microgrid system reliability (MSR) model is developed by integrating the reliability models of wind turbine systems using the system reliability concept. A Monte Carlo simulation technique is utilized to implement the developed reliability models of wind generation and microgrid systems in a Matlab environment. The investigation reveals that maximizing the use of wind generation systems and storage units increases the reliability of power generation of the proposed microgrid system in different operating modes.

Keywords: reliability, microgrid, distributed generation, wind system, modeling and simulation

1. Introduction

Electricity market deregulation, environmental concerns, technology advancement, and an increased trend for reducing the dependency on fossil fuel are the main causes to integrate distributed generation (DG) units into the distribution power network [1, 2]. Generally, DGs have a diverse generation capacity, availability, and primary energy sources. The increasing demand of adding and utilizing such diverse DGs into the distribution power system brought the concept of microgrid. Microgrid is a flexible combination of loads, DG units, storage systems (either centrally or with each generation individually), and associated power conditioning units operating as a single controllable system that provides power or both power and heat to loads [3]. **Figure 1** shows the generic architecture of a microgrid system.

One of the main objectives of having a microgrid system is to supply reliable power to loads in a microgrid domain. The achievement of such an objective becomes critical when a microgrid system consists of renewable energy sources such as wind and/or solar. In the proposed microgrid system, stochastically varying wind creates unpredictable power variation at the output of the wind turbine system. In addition,

IntechOpen

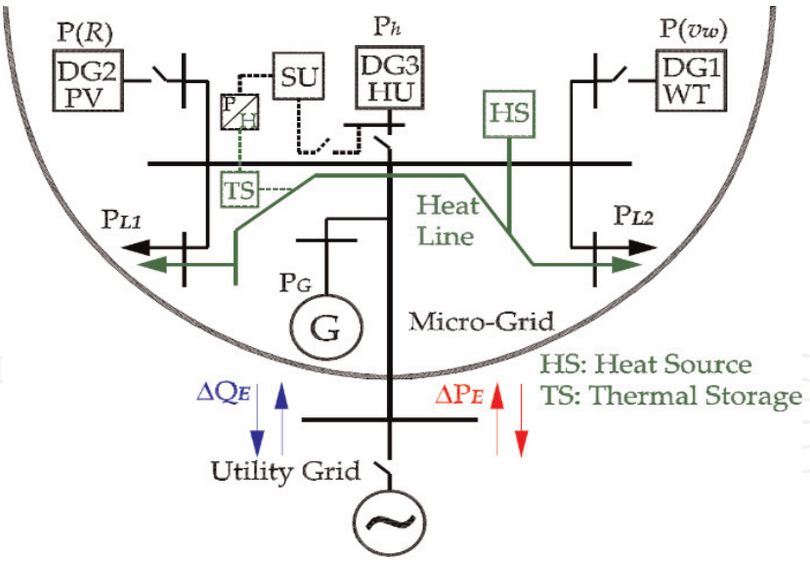


Figure 1.
A generic microgrid system.

such variations in wind speed propagate through all the subsystems in the wind generation system. Therefore, subsystems such as gearbox, generator, and power electronics interfacing units in a wind generation system are also the key factors for producing reliable power by the proposed microgrid system. Thus, it is important to develop the reliability model of the wind generation system including the models of all the subsystems. In addition, consideration of various operation modes of the microgrid system is important to develop a microgrid system reliability model in order to ensure reliable power generation in those operating modes.

The operation, control, and performance characteristics of these microgrids are different because of the contribution of diversity in nature and size of distributed generations in the microgrid. Such diversities of distributed generations include fixed- or variable-speed wind turbines, solar panels, micro-turbines, various types of fuel cells, small hydro, and storage depending upon the sites and resources available. Different control strategies such as load-frequency control, power sharing among parallel converters, central control based on load curve, and active power control are developed for the microgrids presented in [4–15]. The reliability study of a microgrid system is presented in [16], where the concentration is given in a power quality aspect based on the assumption that the microgrid system is a large virtual generator that has the ability to generate sufficient power for loads at various operating conditions. The reliability-based coordination between wind and hydro system is investigated, which shows the adequacy benefits due to the coordination between them when an appropriate number of hydro units are engaged in order to follow the wind speed changes based on the wind power penetration [17].

The reliability and cost assessment of a solar-wind-fuel cell-based microgrid system are investigated in [18]. A recent review study on reliability and economic evaluation of a power system is presented in [19]. It is suggested that the reliability and economic evaluation of power systems with renewable energy sources needs to perform simultaneously. In [20], a new indicator for measuring reliability of a solar-wind microgrid system is showcased. Reliability evaluation of distribution system that consists of wind-storage-photovoltaic system is shown in [21]. It demonstrates the enhancement in reliability of the conventional distribution system using renewable energy sources. In comparison to microgrid architectures and control research, the investigation of the reliability evaluation of microgrid systems has not been much conducted. Therefore, much attention is required to the reliability

evaluation of a microgrid system, which primarily showcases a joined combination of renewable energy sources and storage.

Several researchers have studied the reliability assessment of wind turbine generators in power system applications. The application of two-state and multistate models for wind turbine systems is investigated in [22–24]. However, the stochastic variation and interactions of wind speed and thus time-dependent wind power effects are avoided [25]. A Monte Carlo simulation-based method is then used to assess reliability of a wind generation system in [26–29]. All these past studies evaluate reliability of wind turbine systems by determining the available power output using Eq. (1), while the effect of other subsystems such as gearbox, generator, and interfacing power electronics has not been considered:

$$P_o = \begin{cases} 0 & 0 \le v_w \le v_{ciw} \\ \left(A + Bv_w + Cv_w^2\right)P_r & v_{ciw} \le v_w \le v_{rw} \\ P_r & v_{rw} \le v_w \le v_{cow} \\ 0 & v_w \ge v_{cow} \end{cases} \tag{1}$$

In Eq. (1), P_o and P_r are rotor output power and rated power of the wind turbine, respectively; v_{ciw}, v_{rw}, and v_{cow} are cut-in, rated, and cut-out wind speed, respectively, whereas the parameters A, B, and C are the functions of cut-in, rated, and cut-out wind speeds.

Moreover, these approaches determine available power only at the output of the WT rotor without considering the role of the other subsystems. In [30], reliability evaluation is carried out only for interfacing power electronics subsystems in order to compare performances of small (1.5 kW) wind generation systems. Furthermore, such reliability assessment of the interfacing power electronics sub-system is performed for a single operating point such as the rated wind speed condition. However, operating conditions of a wind generation system normally vary between cut-in and cut-out wind speed due to the stochastic behavior of the wind speed. Hence, the reliability evaluation of generating power by a wind generation system is important to be performed considering the stochastic variation of wind speed as well as the impact of stochastic wind behavior on different subsystems in a wind generation system. Such considerations are essential in order to achieve better reliability estimation and, thus, to ensure reliable power supply by the microgrid system.

The reliability of power generation by a microgrid system consisting of wind generation, hydro generation, and storage unit is evaluated and presented in this chapter. The microgrid system under study is located at Fermeuse, Newfoundland, Canada. The reliability model of the microgrid system is developed by means of a reliability block diagram. Furthermore, reliability models of the subsystems in conjunction with wind speed data modeling are developed and applied. The use of Monte Carlo simulation in a Matlab environment yields the following outcomes:

a. The proposed microgrid system is able to provide reliable power to an isolated microgrid with a minimum number of wind power generation units (only one) with a reliability of 0.94.

b. However, maximizing the use of wind generation unit (as the number increases) improves the microgrid system reliability to provide dependable power to the isolated microgrid.

c. Due to the lack of sufficient wind, the integration of pumped hydro storage increases the microgrid system reliability to ensure reliable power supply to the isolated microgrid system.

2. Microgrid system reliability

The one-line diagram of the case study's microgrid system shown in **Figure 2** consists of a HGU, a WPGS or a wind farm (WF), and two load areas represented as P_{L1} and P_{L2}. HGU and WPGS are apart from each other by a TL1 (20.12) km transmission line.

Microgrid system reliability (MSR) is a measurement of the system's overall ability to produce and supply electrical power. Such measurement indicates the adequacy of power generation and supply by a microgrid system for a given combination of DG units in the system as well as the subsystems contained in a DG unit. In order to evaluate the reliability of the system shown in **Figure 2**, the combination of DG units and the subsystems contained in a DG unit can be presented by means of a reliability block diagram (RBD) [31] as per **Figure 3**.

Owing to the evaluation of the reliability of the generating power supply by the microgrid system, only DG units are considered. As such, the simplified RBD of the microgrid system is presented in **Figure 4**, wherein all DG units are connected in

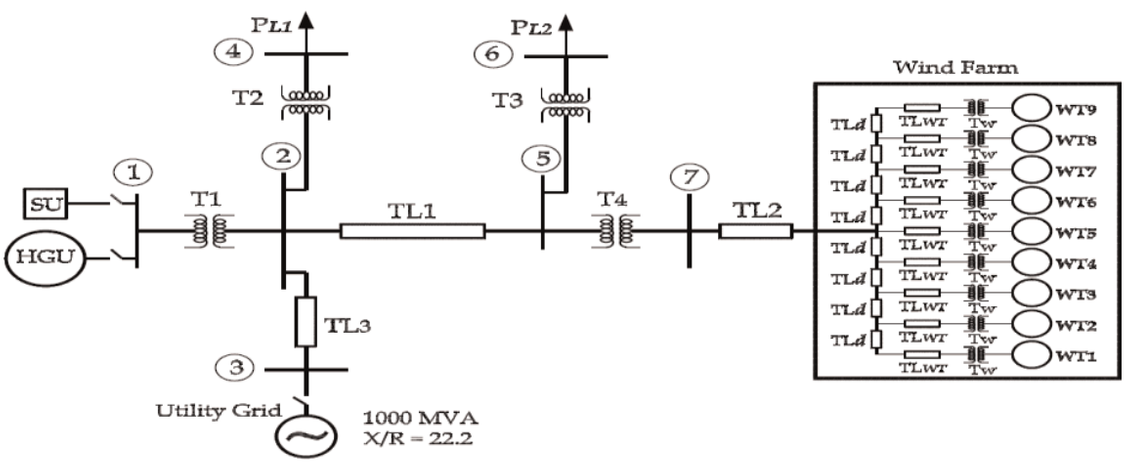


Figure 2.
The single-line diagram of a microgrid system at Fermeuse, Newfoundland, Canada.

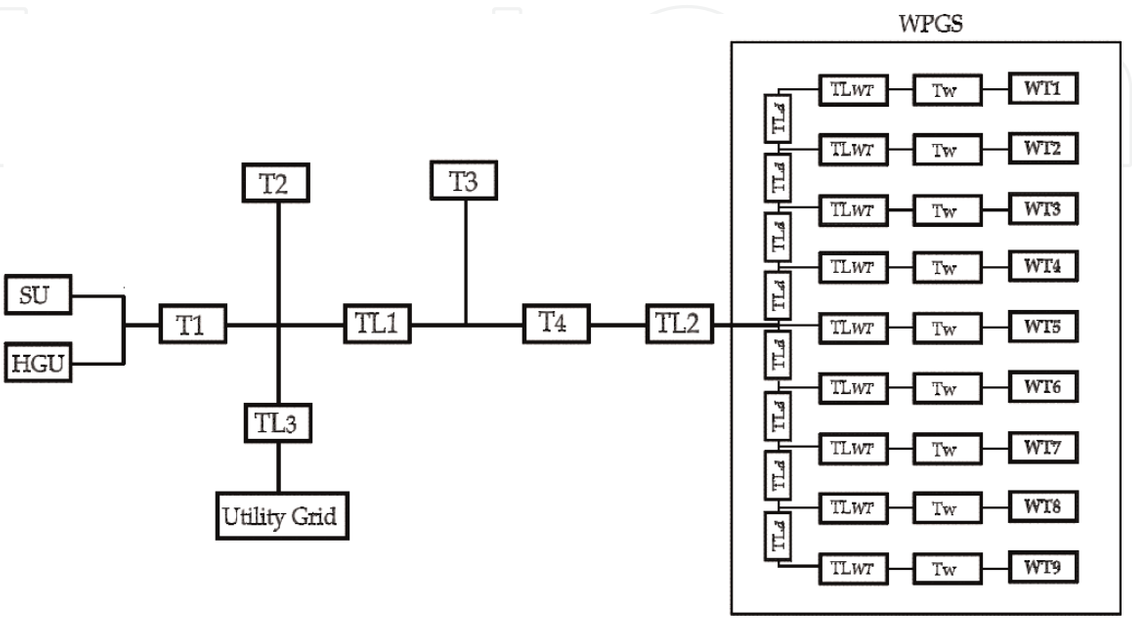


Figure 3.
Detailed reliability block diagram of the microgrid system.

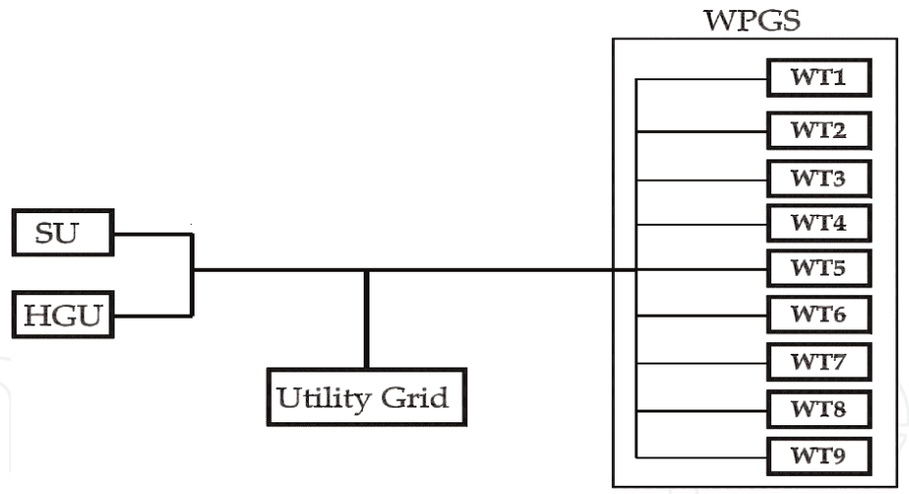


Figure 4.
Simplified reliability block diagram of the microgrid system.

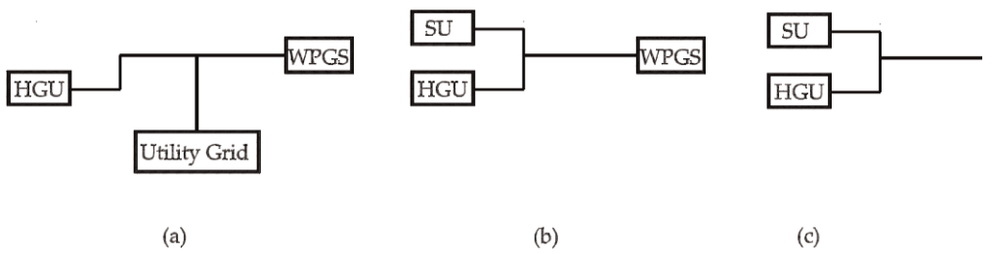


Figure 5.
Reliability block diagram: (a) grid-connected mode, (b) isolated microgrid with wind power generation system, and (c) isolated microgrid without wind power generation system.

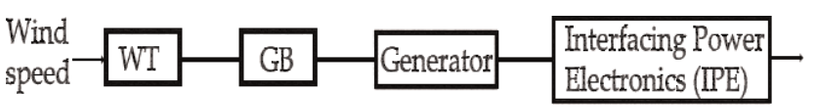


Figure 6.
Reliability block diagram of a wind turbine system.

parallel. However, the RBD of the microgrid system at different operational modes is shown in **Figure 5**.

Moreover, in order to estimate the reliability of a DG unit, its various subsystems may equally be represented by the RBD. The latter is shown in **Figure 6**, which consists of WT or WT rotor, gearbox, generator, and power electronics interfacing circuitry. In this chapter, HGU and utility grid are considered as highly reliable sources of power generation. This is because the HGU at the Fermeuse site produces power at its rated value for an entire year. In addition, the utility grid is also available over the period of a year. The reliability assessment of a storage unit (SU) is beyond the scope of this chapter. However, its reliability is considered based on the fact that the storage system is capable of supplying power to the load during the isolated mode of operation of the microgrid system when wind power generation is unavailable (**Figure 5c**).

3. Reliability modeling

Monte Carlo simulation treats the occurrence of failures as a random event, which mimics the wind speed distribution [32]. For example, in a time series wind

speed data, some of the wind speeds are below the cut-in speed of the wind turbine and, as such, will not produce power at the wind turbine output. Such wind speed data can be considered as failure events, which occur randomly. In addition, this research focuses on assessing the reliability of the microgrid system in power generation and supply, considering the wind speed as the primary uncertainty of the system. Hence, Monte Carlo is applied and presented herein.

3.1 Wind speed data modeling

The relation between wind speed and a WT rotor power output is expressed as [33]

$$P_{ro} = 0.5\rho A_{SA} C_p(\lambda, \beta) v^3 \tag{2}$$

where:

- A_{SA} is the swept area covered by the turbine rotor.
- C_p is the power coefficient.
- v_w is the wind velocity.
- β is the pitch angle of rotor blades.
- λ is the tip speed ratio.
- ρ is the air density. Note that for a given WT, A_{SA}, Cp, β, λ, and ρ are constant.

The relation in Eq. (2) can be expressed as

$$P_{ro} \infty v_w^3 \tag{3}$$

Since wind speed is the main factor that creates uncertainty at the power output of a wind energy conversion, wind speed is considered here as the key factor to estimate the MSR. In order to relate the effects of wind speed in calculating the system's overall reliability, wind speed field data modeling is gathered. This is essential because the data itself varies not only from site to site but also according to the hub heights of the wind turbine. Wind speed data modeling for a wind turbine system includes:

a. Identifying best-fit distribution for 1-year wind field data

b. Evaluating the goodness-of-fit test

c. Estimating the distribution parameters

3.1.1 Identification of best-fit distribution

The probability plot method is used to identify the best-fit distribution of the available wind data for a given site and for a given wind turbine hub height. The following steps are taken to accomplish the fitting of the wind data to a distribution:

- Obtain 1-year wind speed data from the site measurement.
- Scale the wind data according to the hub height of the wind turbine using Eq. (4):

$$v_{w2} = v_{w1}\left(\frac{h_2}{h_1}\right)^{\alpha} \tag{4}$$

where h_1 and h_2 are the height of anemometer and hub, respectively; v_{w1} and v_{w2} are the wind velocity at anemometer height and at hub height, respectively; and α is the shear exponent that is expressed as

$$\alpha = (0.096\log(Z_o) + 0.016\log(Z_o))^2 + 0.24 \tag{5}$$

where Z_0 is the surface roughness.

- Use Matlab distribution fitting tool to obtain probability plot of the scaled wind data.
- Fit the probability plot of the scaled wind data for different distributions such as normal, log-normal, exponential, and Weibull.
- Identify the distribution corresponding to the best fit of the probability plots.

3.1.2 Goodness-of-fit test

The best-fit distribution of the site wind data is tested for the goodness-of-fit and is performed according to the statistic for MANN'S test:

$$M = \frac{k_1\sum_{i=k_1+1}^{r-1}\left[\left(\ln\left(v_{w_{i+1}}\right) - \ln\left(v_{w_i}\right)\right)/M_i\right]}{k_2\sum_{i=1}^{k_1}\left[\left(\ln\left(v_{w_{i+1}}\right) - \ln\left(v_{w_i}\right)\right)/M_i\right]} \tag{6}$$

3.1.3 Distribution parameter estimation

To determine the Weibull distribution parameters, the least-squares technique is used because of its accuracy to fit a straight line in a given data points. In this approach, the wind speed field data are transformed to Weibull distribution to fit to a linear regression line as in Eq. (7):

$$y_i = a + bx_i \tag{7}$$

where

$$x_i = \ln v_{wi} \tag{8}$$

$$y_i = Z_i \tag{9}$$

$$a = -\beta_{ws}\ln\theta \tag{10}$$

$$b = \beta_{ws} \tag{11}$$

The values of a and b are determined from the least-squares fit using Eqs. (8) and (9).

By knowing the values a and b, the Weibull parameters are determined as follows:

$$\theta_{ws} = \exp\left(-\frac{a}{b}\right) \tag{12}$$

$$\beta_{ws} = b \tag{13}$$

where θ_{ws} and β_{ws} are defined as the scale and shape parameters, respectively, for wind speed field data.

3.2 Wind power generation system

According to the microgrid configuration, all nine WTs in WPGS are connected in parallel, which are shown in the simplified RBD in **Figure 4**. In order to estimate the reliability of power generation by the WPGS, a single WT system is considered because all of them are identical both in terms of topology and subsystems context. A WT system comprising of different subsystems is shown in **Figure 6**. The different subsystems are connected in series because failure of power generation by any of the subsystems is considered as a failure of the WT system to generate power. The modeling of the reliability estimation of different subsystems in a WT system is described in the following subsections:

3.2.1 Wind turbine rotor

The wind speed field data model provides information about the shape parameter and scale factor for a Weibull distribution. Such parameters are used to generate a series of random wind speed data that follow a Weibull distribution pattern. Randomly generated data are used to determine power generation by the WT using Eq. (2), which represents a Weibull distribution of power generation. Weibull parameters are determined using the parameter estimation technique described in Section 3.1. These are defined as θ_{tp} and β_{tp}. Thus, the WT's rotor reliability R_{tp} can be expressed as

$$R_{tp} = \exp\left[-\left(\frac{P_{ciw}}{\theta_{tp}}\right)^{\beta_{tp}}\right] - \exp\left[-\left(\frac{P_{cow}}{\theta_{tp}}\right)^{\beta_{tp}}\right] \tag{14}$$

where θ_{tp} and β_{tp} are defined as shape parameter and scale factor for power distribution. P_{ciw} and P_{cow} are the power at cut-in and cut-out wind speed, respectively.

The reliability of generating power at the *ith* wind speed, R_{Pi}, can be expressed as

$$R_{Pi} = \exp\left[-\left(\frac{P_i}{\theta_{tp}}\right)^{\beta_{tp}}\right] \tag{15}$$

where P_i is the power for *ith* wind speed in between cut-in and cut-out regions.

3.2.2 Gearbox

Weibull parameters obtained from field data modeling are utilized to produce a set of random wind data. Such data are used to determine the wind turbine speed using Eq. (16):

$$\omega_{wt} = \frac{\lambda v_w}{R_t} \tag{16}$$

where ω_{wt} is the wind turbine speed and R_t is the turbine radius, respectively. The wind turbine speed is also the speed seen by the gearbox's low-speed shaft. This can be represented as a Weibull distribution of speed. Such a distribution is utilized

to estimate the shape parameter and the scale factor of the gearbox. Its reliability R_{gb} can be expressed as

$$R_{gb} = \exp\left[-\left(\frac{\omega_{wt,s}}{\theta_{gb}}\right)^{\beta_{gb}}\right] - \exp\left[-\left(\frac{\omega_{wt,m}}{\theta_{gb}}\right)^{\beta_{gb}}\right] \tag{17}$$

where:

- $\omega_{wt,s}$ is the starting speed of the wind turbine.
- θ_{gb} and β_{gb} are the shape parameter and scale factor for speed seen by the gearbox.
- $\omega_{wt,m}$ is the maximum operating speed of the wind turbine.

The reliability at the *ith* speed seen by the gearbox, $R_{gb,wti}$, can be estimated as

$$R_{gb_{wt,i}} = \exp\left[-\left(\frac{\omega_{wt,i}}{\theta_{gb}}\right)^{\beta_{gb}}\right] \tag{18}$$

where $\omega_{wt,I}$ is the *ith* speed of the WT seen by the gearbox.

3.2.3 Generator

In order to account the effect of wind speed in estimating the wind generator's reliability of generating power, the estimation of Weibull parameters by using field data is shown herein. Such parameters are utilized to generate a set of random wind speed data. Power generated by the WT is then determined using Eq. (2). However, the power at the generator output depends on the gearbox efficiency and various losses in the generator. Efficiency of the gearbox (0.95) and generator (0.95) is considered as 90%, which is observed from the system modeling and simulation. The power at the generator output can be determined as 90% of the power at the turbine output. Thus, a power distribution at the generator output can be obtained, which also follows a Weibull distribution. This, in turn, is used to estimate Weibull distribution parameters using the least-squares parameter estimation technique. After knowing the distribution parameters of the generator output power, the reliability of generating power by the generator, R_g, can be evaluated as

$$R_g = \exp\left[-\left(\frac{P_{g,ciw}}{\theta_{gp}}\right)^{\beta_{gp}}\right] - \exp\left[-\left(\frac{P_{g,cow}}{\theta_{gp}}\right)^{\beta_{gp}}\right] \tag{19}$$

where:

- θ_{gp} and β_{gp} are considered as shape parameter and scale factor for the generator power distribution.
- $P_{g,ciw}$ and $P_{g,cow}$ are the generator power at the cut-in and cut-out wind speeds, respectively.

The reliability of generating power $P_{g,i}$ of the generator, $RP_{g,i}$, can be expressed as

$$R_{P_{g,i}} = \exp\left[-\left(\frac{P_{g,i}}{\theta_{gp}}\right)^{\beta_{gp}}\right] \tag{20}$$

where $P_{g,I}$ is the generator power at the *ith* wind speed in between cut-in and cut-out regions.

3.2.4 Power electronics interfacing system

An interfacing power electronics (IPE) system in a doubly fed induction generator-based WT consists of a back-to-back pulse width modulated (PWM) converter as shown in **Figure 7**. The components in the IPE system are diodes, IGBT switches, and a DC bus capacitor. The reliability model of such a system can be developed based on the relationship between the lifetime and failure rate of the components in the system. These are determined considering the junction temperature as a covariate. The junction temperature, T_j, of a semiconductor device can be calculated as [34]

$$T_j = T_a + P_l R_{ja} \tag{21}$$

where P_l, T_a, and R_{ja} are the power loss of a component, the ambient temperature, and the junction resistance, respectively. A reliability model of a power conditioning system for a small (1.5 kW) wind energy conversion system is developed by considering power loss only at a rated wind speed operating condition.

However, it is to be noted that power losses in the semiconductor components vary according to the wind speed variation at the wind turbine input. Thus, a power loss variation in the semiconductor component is important to be considered as a stress factor in order to calculate the lifetime of the components instead of using power loss quantity for a single operating condition. Hence, Eq. (21) can be expressed as

$$T_{j_i} = T_a + P_{l_i} R_{ja} \tag{22}$$

where:

- P_{l_i} is the power loss of a component at the i^{th} wind speed.
- T_{j_i} is the component junction temperature at the i^{th} wind speed
- Junction resistance is assumed to be constant for all wind speed.

In an IPE system, there are two types of semiconductor components, namely, diode and IGBT switches. Two types of power losses such as conduction losses and switching losses occur in such components. The conduction loss, $P_{cl,d}$, and the switching loss, $P_{sl,d}$, of a diode can be expressed as [35, 36]

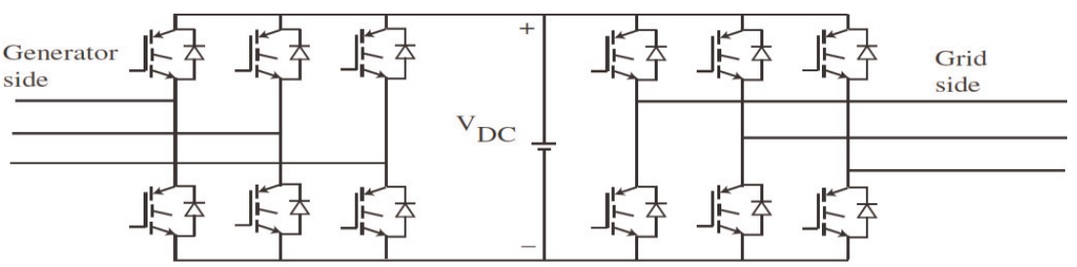


Figure 7.
Interfacing power electronics system of a doubly fed induction generator-based wind turbine system.

$$P_{cl,d} = \left(\frac{1}{8} - \frac{M}{3\pi}\cos\varphi\right)R_d I_{mo}^2 + \left(\frac{1}{2\pi} - \frac{M}{8}\cos\varphi\right)V_{FO} I_{mo} \tag{23}$$

$$P_{sl,d} = \frac{1}{\pi} f_s E_{sr} \frac{V_{dc} I_{mo}}{V_{ref,d} I_{ref,d}} \tag{24}$$

Total power losses of diodes, $P_{tl,d}$, in the IPE system can be expressed as the sum of the conduction loss, $P_{cl,d}$, for the total number of diodes. The switching loss, $P_{sl,d}$, for the total number of switches in the system can be expressed as

$$P_{tl,d} = n\left(\frac{1}{8} - \frac{M}{3\pi}\cos\varphi\right)R_d I_{mo}^2 + n\left(\frac{1}{2\pi} - \frac{M}{8}\cos\varphi\right)V_{FO} I_{mo} + n\frac{1}{\pi} f_s E_{sr} \frac{V_{dc} I_{mo}}{V_{ref,d} I_{ref,d}} \tag{25}$$

where:

- M is the modulation index ($0 \le M \le 1$).
- I_{mo} is maximum output current of the inverter.
- n is the number of semiconductor components.
- V_{FO} and R_d are the diode threshold voltage and resistance, respectively.
- f_s is the switching frequency.
- E_{er} is the rated switching loss energy given for the commutation voltage.
- $V_{ref,d}$ and $I_{ref,d}$, V_{dc}, and I_{dc} are the actual commutation voltage and current, respectively.
- φ is the angle between voltage and current.

The conduction loss, $P_{cl,IGBT}$, and switching loss $P_{sl,IGBT}$ of an IGBT switch can be expressed as [37]

$$P_{cl,IGBT} = \left(\frac{1}{8} + \frac{M}{3\pi}\cos\varphi\right)R_{ce} I_{mo}^2 + \left(\frac{1}{2\pi + \frac{M}{8}\cos\varphi}\right)V_{CEO} I_{mo} \tag{26}$$

$$P_{sl,IGBT} = \frac{1}{\pi} f_s \left(E_{on} + E_{off}\right) \frac{V_{dc} I_{mo}}{V_{ref,IGBT} I_{ref,IGBT}} \tag{27}$$

Total power losses of switches, $P_{tl,IGBT}$, in the IPE system can be expressed as the sum of the conduction loss, $P_{cl,IGBT}$, for total number of diodes. The switching loss, $P_{sl,IGBT}$, for the total number of switches in the system can be expressed as

$$P_{tl,IGBT} = n\left(\frac{1}{8} + \frac{M}{3\pi}\cos\varphi\right)R_{ce} I_{mo}^2 + n\left(\frac{1}{2\pi} + \frac{M}{8}\cos\varphi\right)V_{CEO} I_{mo} + n\frac{1}{\pi} f_s \left(E_{on} + E_{off}\right) \frac{V_{dc} I_{mo}}{V_{ref,IGBT} I_{ref,IGBT}} \tag{28}$$

where:

- V_{CEO} and R_{ce} are the IGBT threshold voltage and on-state resistance, respectively.

- The reference commutation voltage and current are $V_{ref,IGBT}$ and $I_{ref,IGBT}$.
- V_{dc} is the actual commutation voltage.
- E_{on} and E_{off} are the turn-on and turn-off energies of IGBT.

The lifetime, $L(T_{ji})$, of a component for *ith* wind speed can be expressed as

$$L(T_{ji}) = L_o \exp\left(-B\Delta T_{ji}\right) \tag{29}$$

where:

- L_o is the quantitative normal life measurement (assumed to be 10^6).
- $B = \frac{E_A}{K}$, where K is the Boltzmann's constant (=8.6 $\times$ 10^{-5} eV/K) and E_A is the activation energy (= 0.2 eV) for typical semiconductor components.
- ΔT_{ji} is the variation in junction temperature for the *ith* wind speed and can be expressed as

$$\Delta T_{ji} = \frac{1}{T_a} - \frac{1}{T_{ji}} \tag{30}$$

The failure rate of a component for *ith* wind speed can be defined as

$$\tau_i = \frac{1}{L(T_{ji})} \tag{31}$$

Using Eq. (31), a distribution of failure rates for a set of wind speed data for a semiconductor component can be generated. The components in the IPE system are considered as an in-series connection from the reliability point of view, because the IPE system fails, if any one of the components breaks down in the IPE system. Thus, the failure rates for different components are added to determine the failure rate of the IPE system for the *ith* wind speed. Hence, a distribution of failure rates for the IPE system can be generated for a series of wind speed data.

A least-squares technique is then used to determine the distribution parameters. By knowing the distribution parameters, the reliability of the IPE system, R_{IPE}, can be modeled as

$$R_{IPE} = \exp\left[-\left(\frac{\tau_{ciw}}{\theta_{IPE}}\right)^{\beta_{IPE}}\right] - \exp\left[\left(\frac{\tau_{cow}}{\theta_{IPE}}\right)^{\beta_{IPE}}\right] \tag{32}$$

Hence:

- θ_{IPE} and β_{IPE} are defined as the shape parameter and the scale factor for the failure rate distribution of the IPE system.
- τ_{ciw} and τ_{cow} are failure rates of IPE system at cut-in and cut-out wind speeds, respectively.

The reliability of a component in IPE system, R_{IPEC}, can be expressed as

$$R_{IPE_C} = \exp\left[-\left(\frac{\tau_{ciw_C}}{\theta_{IPE_C}}\right)^{\beta_{IPE_C}}\right] - \exp\left[\left(\frac{\tau_{cow_C}}{\theta_{IPE_C}}\right)^{\beta_{IPE_C}}\right] \tag{33}$$

where:

- θ_{IPE_C} and β_{IPE_C} are defined as the shape parameter and the scale factor for the failure rate distribution of a component.

- τ_{ciw_C} and τ_{cow_C} are failure rates at cut-in and cut-out wind speeds for a component, respectively.

The reliability of a WT system, R_{wts}, can now be expressed as

$$R_{wts} = R_{tp} \times R_{gb} \times R_g \times R_{IPE} \tag{34}$$

In WPGS, all nine WTs are connected in parallel with identical configuration. Hence, the reliability of the WPGS, R_{WPGS}, can be expressed as

$$R_{WPGS} = \left[1 - (1 - R_{wts})^N\right] \tag{35}$$

where N is the number of WT system in a WPGS.

3.3 Microgrid reliability model

Figure 4 shows the simplified RBD of the microgrid system, where all DG units are connected in parallel. In addition, SU is considered as a power-generating unit since it will supply power to the load during an isolated mode of operation of the microgrid. Assuming the reliability of the HGU as R_{HGU} and utility grid as R_{UG}, the overall microgrid system reliability, R_{MSR}, can be modeled as

$$R_{MSR} = \left[1 - (1 - R_{wts})^N (1 - R_{HGU})(1 - R_{UG})\right] \tag{36}$$

However, the microgrid system operates in three different modes, which are shown in **Figure 5**. The MSR can also be modeled according to their operating modes. **Figure 5a** shows the grid-connected mode of operation where all DG or generation units are connected with the utility grid. Thus, the MSR pertaining to the grid-connected mode of operation, $R_{MSR_{M1}}$, can be expressed by the similar model presented in Eq. (36). Therefore,

$$R_{MSR_{M1}} = \left[1 - (1 - R_{wts})^N (1 - R_{HGU})(1 - R_{UG})\right] \tag{37}$$

Figure 5b represents an isolated microgrid system with WPGS. In addition, the storage unit is not working as a generation unit in this mode of operation. Thus, the MSR during isolated operation with WPGS, $R_{MSR_{M2}}$, can be defined as

$$R_{MSR_{M2}} = \left[1 - (1 - R_{wts})^N (1 - R_{HGU})\right] \tag{38}$$

Furthermore, **Figure 5c** shows an isolated microgrid without WPGS mode where the SU operates as a generation unit. Assuming that the reliability of the SU is R_{SU}, hence, the MSR during this mode, $R_{MSR_{M3}}$, can be written as

$$R_{MSR_{M3}} = [1 - (1 - R_{HGU})(1 - R_{HGU})] \tag{39}$$

4. Implementation of the microgrid model

In order to implement the developed MSR model so as to evaluate the power generation reliability of the proposed microgrid system, Monte Carlo simulation is performed using Matlab. The flow diagram is shown in **Figure 8** and is explained in steps 1–5. The model of the MSR and the reliability evaluation of various operating modes of the proposed microgrid are implemented using Matlab code according to the flow chart shown in **Figure 9** and explained in steps 6–7.

Step 1: Wind speed field data model

- Field data collection and distribution identification using probability plots
- Goodness-of-fit test for selecting the distribution of wind speed
- Calculating the distribution parameter using Eqs. (12) and (13)
- Generating a series of random data as the input for the next steps of the reliability flow diagram

Step 2: Reliability of power generation by WT rotor

- WT rotor output power distribution generation

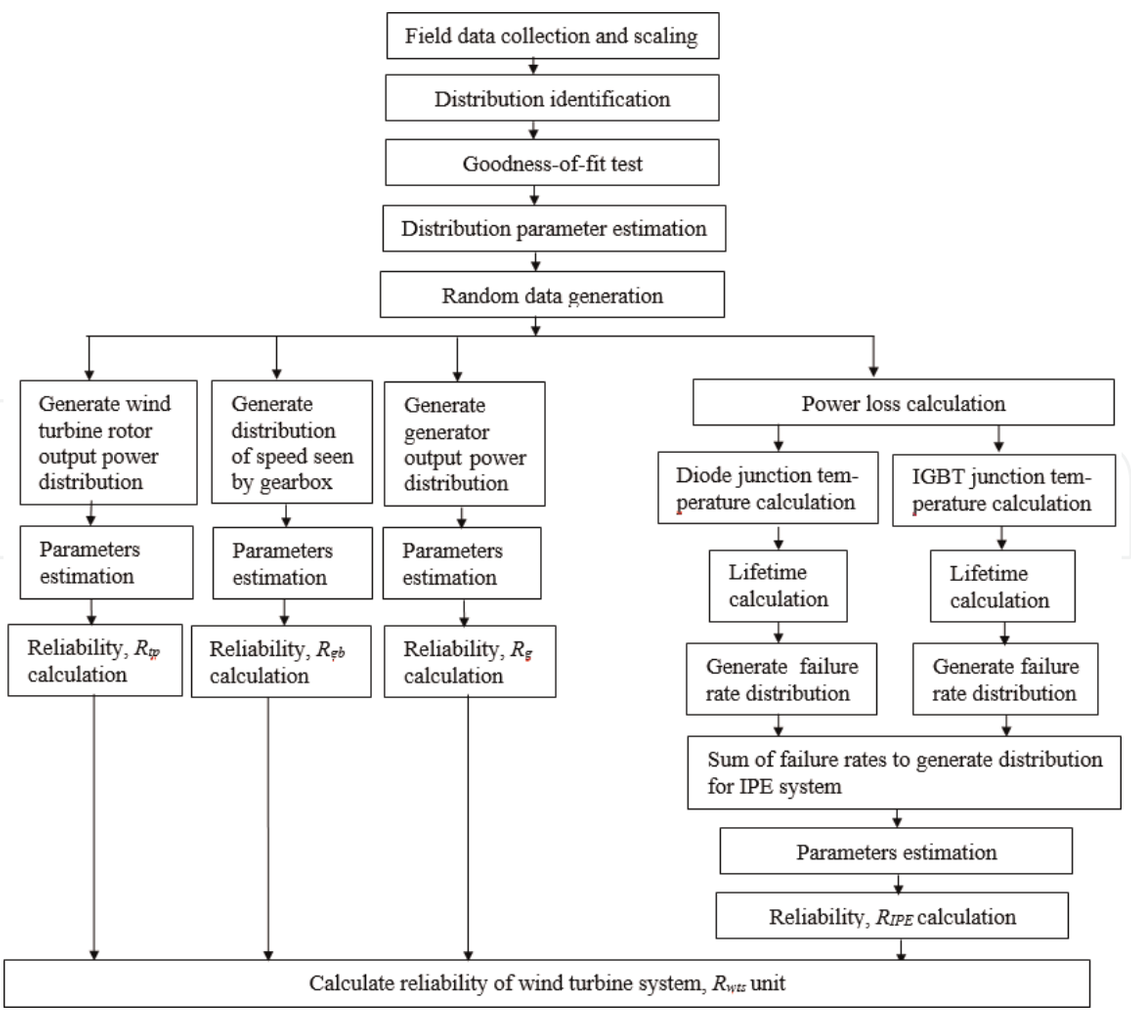


Figure 8.
Flow diagram for reliability calculation of wind generation subsystems.

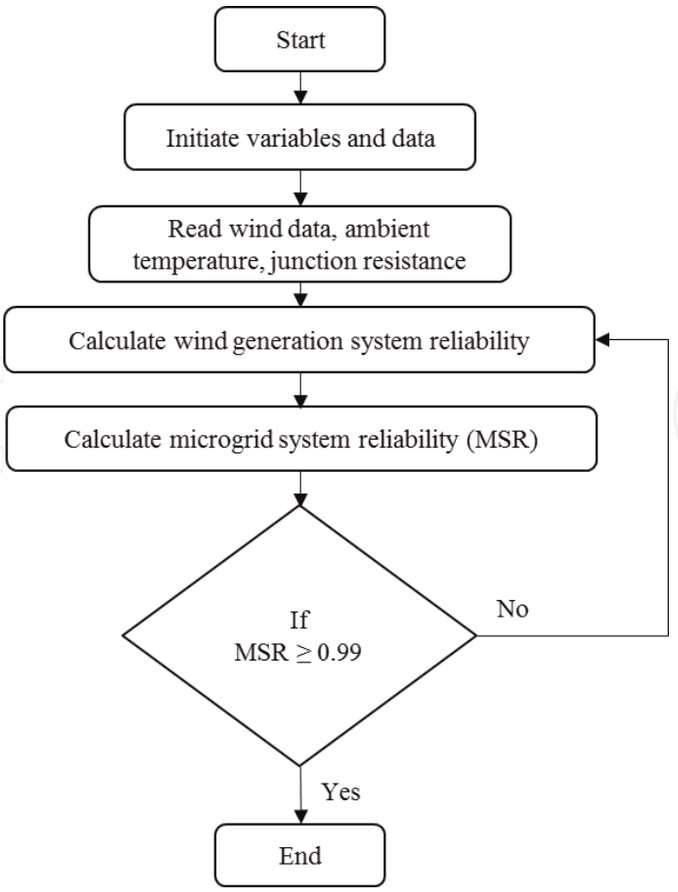


Figure 9.
Flow chart for calculating the microgrid system reliability.

- Parameter estimation for WT rotor power distribution
- Reliability calculation using Eq. (14)

Step 3: Reliability of gearbox

- Determining speed distribution seen by the gearbox
- Speed distribution parameter calculation using least-squares technique
- Reliability calculation using Eq. (17)

Step 4: Reliability of generator

- Generator output power distribution generation
- Distribution parameter determination using least-squares technique
- Reliability evaluation of generator output power using Eq. (19)

Step 5: Reliability of interfacing power electronics

- Power loss calculation of diodes and IGBTs in the IPE system using Eqs. (25) and (28)
- Failure rate distribution generation for diodes and IGBT switches

- Estimating parameter of failure rate distribution of IPE system
- Calculating reliability using Eq. (32)

Step 6: Reliability of DG units

- Reliability calculation of a WT system using Eq. (34)
- Determining reliability of WPGS using Eq. (35)
- Assuming reliability for HGU and SU

Step 7: Reliability of microgrid system

- MSR calculation using Eqs. (36)–(39) for various operational modes

5. Simulation results

The reliability model and its implementation procedure described in the preceding sections are performed to determine probability distribution parameters as well as the reliability of the various subsystems in the wind generation system for stochastically varying wind speed condition. Such reliability estimation is then utilized to determine MSR in various operating modes of the microgrid. The power generation wind speed region of the selected turbine is v_{ciw} = 4 m/s and v_{cow} = 25 m/s. The reliability of HGU and utility grid are selected as 85%, since they are regarded as highly reliable power generation sources. The reliability of the storage unit is assumed to be the same as the IPE system (=0.8144), because these are commonly interfaced through power electronics inverter systems. One-year wind speed data is used for the field data modeling process. Assume that three WT systems can be connected to the isolated microgrid system due to the stability issue.

Figure 10 shows the hourly wind speed field data collected over a 1-year period. Such data is utilized to identify the distribution using probability plot techniques. The probability plots of wind speed field data are shown in **Figure 11**, revealing that the probability of wind speed follows Weibull and Rayleigh distributions closely. However, the Weibull distribution follows the probability of wind speed closer than the Rayleigh distribution. Thus, the Weibull distribution is identified as the best-fit distribution for wind speed data in this study. In order to select Weibull distribution, a goodness-of-fit test is also carried out, and the probability density function of Weibull distribution is shown in **Figure 12**.

A least-squares method is performed to estimate the Weibull distribution parameter, which is shown in **Figure 13**. The shape parameter for wind speed

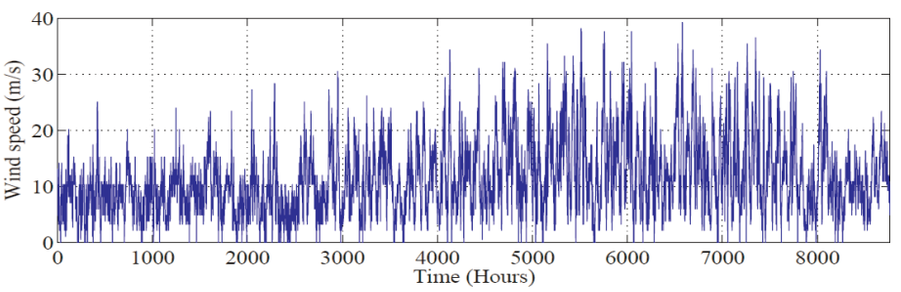


Figure 10.
Wind speed field data.

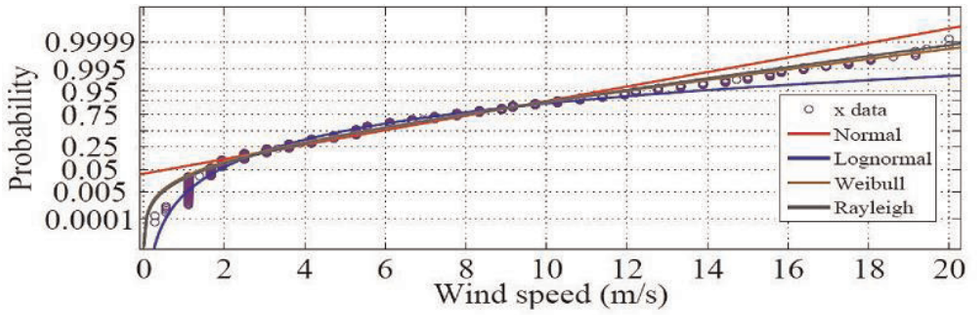


Figure 11.
Probability plots for distribution identification.

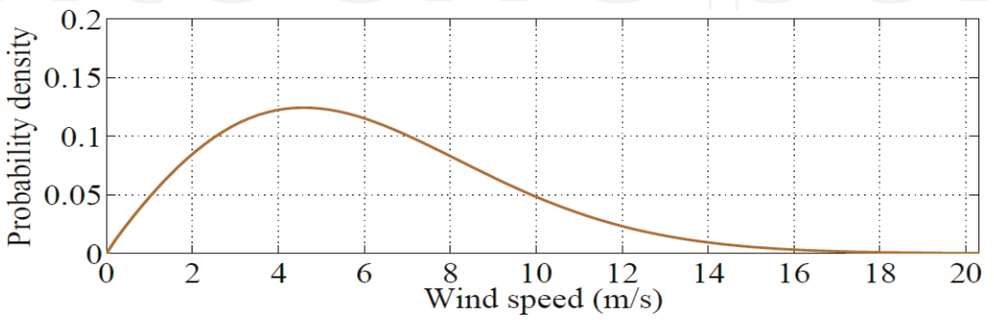


Figure 12.
Probability density function of wind speed data.

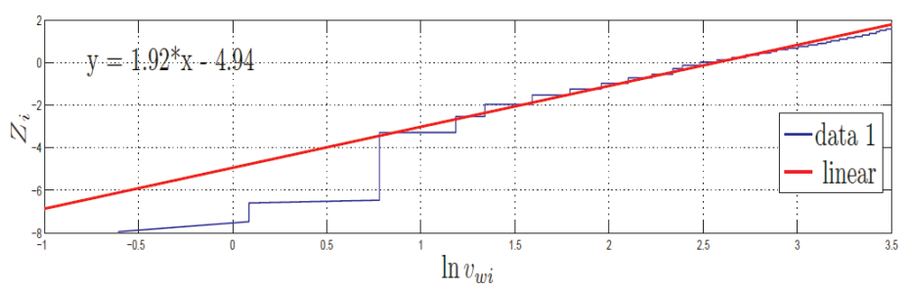


Figure 13.
Least-squares plot for parameter estimation.

β_{ws} = 1.92, and the scale parameter θ_{ws} = 13.1. These parameters are used to generate random wind speed data for reliability evaluation of different subsystems in a wind turbine system.

The results of the reliability calculation for different subsystems in a wind generation system are presented in **Table 1**. The outcomes reveal that the resulting reliability of the wind turbine rotor is 0.9068, while the reliability of gearbox and generator are 0.9107 and 0.9266, respectively. However, the reliability of generating power for the IPE sub-system is only 0.8144. These findings indicate that the IPE sub-system in a variable-speed wind generator system is less reliable than the other subsystems. **Table 2** presents the reliability results of DG units such as WT system, WPGS, HGU, SU, and utility grid. The reliability of a WT system and a WPGS is calculated based on the model derived in this study; however, the reliability of HGU, SU, and utility grid is assumed based on their availability in operation. The overall reliability of a wind turbine system is 0.6232. Since nine WT systems are connected in parallel in the WPGS, the calculated reliability of WPGS is significantly high.

The reliability estimation results of the microgrid system during various operational modes are presented in **Table 3**. The MSR during grid-connected mode is

Sub-systems	Distribution parameters		Sub-systems parameters		Reliability
WT rotor	θ_{tp}	β_{tp}	P_{ciw}	P_{cow}	R_{tp}
	1560.58	1.422	77	3000	0.9068
Gearbox	θ_{gb}	β_{gb}	$\omega_{wt,s}$	$\omega_{wt,\mathrm{m}}$	R_{gb}
	13.73	3.33	4.1	18.4	0.9107
Generator	θ_g	β_g	$P_{g,ciw}$	$P_{g,cow}$	R_g
	1354	1.4142	73	2850	0.9266
IPE system	θ_{IPE}	β_{IPE}	τ_{ciw}	τ_{cow}	R_{IPE}
	1.158	2.658e-5	0.0202e-4	0.4821e-4	0.8144

Table 1.
Reliability results of different subsystems in a variable-speed wind generator system.

DG units	Reliability	DG units	Reliability
WT system	R_{wts}	HGU	R_{HGU}
	0.6232		0.85
WPGS	R_{WPGS}	SU	R_{SU}
	0.9998		0.8144

Table 2.
Reliability results of distributed generation units.

Microgrid operational modes	Reliability
Grid-connected mode	$R_{MSR_{M1}}$
	0.9999
Isolated microgrid with WPGS: number of WTs in WPGS (1, 2, 3, 4)	$R_{MSR_{M2}}$
	0.94, 0.97, 0.99, 0.997
Isolated microgrid without WPGS	$R_{MSR_{M3}}$
	0.99

Table 3.
Reliability results of microgrid system.

higher than the other operational modes because all DG units are operating during this mode. Moreover, this mode has two generation sources which are assumed as highly reliable in power generation and supply.

On the other hand, MSR during isolated microgrid with WPGS varies depending on the number of WT system operating in the WPGS. It is worth mentioning that in an isolated microgrid system, all WTs in WPGS do not operate due to stability issues. This issue will occur since all WTs in WPGS will require reactive power for their operation during isolated mode. However, in an isolated mode, there is no such reactive power generation source to provide sufficient reactive power for all nine WT systems. Thus, the reliability calculation is carried out for a different number of WT systems in the WPGS, and the various reliability indices are found. On the other hand, it is important to note that the minimum reliability index found is 0.94, which is high.

Moreover, the reliability level during this mode of operation (**Figure 5b**) can also be increased by adding more generation sources within the maximum number of constraint (maximum number of WT system).

The reliability of the microgrid system without WPGS is calculated as 0.97, which is higher than that of a microgrid system with WPGS. This is due to the combination of generation sources in this mode of operation (**Figure 5c**), which are highly reliable than the generation source (such as WT) in the WPGS. The results of the reliability evaluation shows that the proposed microgrid system has the significant ability to generate sufficient power to ensure the reliable power supply in all operating modes. The reliability indices found in this study reveal that a microgrid system consisting of renewable energy sources such as wind, hydro, and storage is reliable in generating and supplying power.

6. Conclusions

This chapter discussed the reliability assessment of a microgrid system, comprising variable-speed wind generator units. This research was carried out on a microgrid system located at Fermeuse, Newfoundland, Canada. The mathematical model of microgrid system reliability is developed based on the reliability block diagram (RBD) concept. In addition, the reliability model of various subsystems in a variable-speed wind generator unit is developed considering the impact of stochastically varying wind speed. The developed microgrid system reliability model is implemented through Monte Carlo simulation using Matlab coding. The obtained results are presented and discussed.

- The reliability performance of generating and supplying reliable power by the case study microgrid system during its various operational modes is found to equal 0.99 (grid-connected mode), 0.99 (isolated microgrid with WPGS), and 0.99 (isolated microgrid without WPGS).

- This suggests that the microgrid has the ability to generate and supply power to the loads in a microgrid domain with a high degree of reliability. Such a reliability level is achieved due to maximizing the use of renewable power. The latter stems from wind generation systems as well as storage units.

- It is the authors' view that this reliability evaluation approach may be applied to assess the reliability of microgrid systems containing other intermittent energy sources such as solar.

The developed and presented method in this chapter is implemented using simulation. However, this method is neither implemented in real time, nor is it sold to industry yet. This method needs further investigation to include other renewable sources such as solar-based ones. In addition, an experimental investigation is also required, which in turn may prove challenging, as a number of key issues need to be addressed.

At present, the author is further researching the possibility of applying described method for a microgrid that consists of a solar photovoltaic system and may be applicable to hot weather conditions.

Acknowledgements

This work is supported by a research grant from the National Science and Engineering Research Council (NSERC) of Canada, the Atlantic Innovation Fund

(AIF) of Canada, and Memorial University of Newfoundland. The author also would like to acknowledge the utility company, Newfoundland Power, Canada, for providing the system information and data.

Conflict of interest

There is no conflict of interest.

Abbreviations

DC	direct current
DG	distributed generation
GB	gearbox
HGU	hydro generation unit
IGBT	insulated-gate bipolar transistor
IPE	interfacing power electronics
MSR	microgrid system reliability
PWM	pulse width modulation
RBD	reliability block diagram
SU	storage unit
WF	wind farm
WPGS	wind power generation system
WT	wind turbine

Author details

Razzaqul Ahshan
Department of Electrical and Computer Engineering, Sultan Qaboos University, Muscat, Sultanate of Oman

*Address all correspondence to: razzaqul@squ.edu.om

IntechOpen

© 2019 The Author(s). Licensee IntechOpen. This chapter is distributed under the terms of the Creative Commons Attribution License (http://creativecommons.org/licenses/by/3.0), which permits unrestricted use, distribution, and reproduction in any medium, provided the original work is properly cited. CC BY

References

[1] Ahshan R, Iqbal MT, Mann GKI, Quaicoe JE. Modeling and analysis of a micro-grid system powered by renewable energy sources. The Open Renewable Energy Journal. 2013;**6**:7-22

[2] Ahshan R, Shafiq M, Hosseinzadeh N, Al-Badi A. Distributed wind systems for moderate wind speed sites. In: 5th Int. Conf. on Renewable Energy Generation and Applications; UAE: Al-Ain; 2018

[3] Lasseter RH. Microgrids. In: Proc. of IEEE Power Engineering Society Winter Meeting; 2002. pp. 1-4

[4] Barnes M, Dimeas A, Engler A, Fitzer C, Hatziargyriou N, Jones C, et al. Microgrid laboratory facilities. In: IEEE International Conference on Future Power System; 2005

[5] Lopes JAP, Madureira AG, Moreira CCLM. A view of microgrids. WIREs Energy and Environment. 2013;**2**: 86-103. DOI: 10.1002/wene.34

[6] Hatziargyriou N, Asano H, Iravani MR, Marnay C. Microgrids—An overview of ongoing research, development and demonstration projects. In: IEEE Power and Energy Magazine, LBNL-62937; 2007. pp. 78-94

[7] Morozumi S. Overview of microgrid research and development activities in Japan. In: IEEE Symposium on Micro-grids; 2006

[8] Katiraei F, Iravani MR, Lehn PW. Small signal dynamic model of a microgrid including conventional and electronically interfaced distributed resources. IET Generation Transmission and Distribution. 2007;**1**(3):369-378

[9] Katiraei F, Abbey C, Bahry R. Analysis of voltage regulation problem for 25kV distribution network with distributed generation. In: Proc. of IEEE Power Engineering Society General Meeting; 2006. pp. 1-8

[10] Ibrahim H, Ghandour M, Dimitrova M, Ilinca A, Perron J. Integration of wind energy into electricity systems: Technical challenges and actual solutions. Energy Procedia. 2011;**6**: 815-824

[11] Shahabi M, Haghifam MR, Mohamadian M, Nabavi-Niaki SA. Microgrid dynamic performance improvement using a doubly fed induction wind generator. IEEE Transactions on Energy Conversion. 2009;**24**(1):137-145

[12] Majumder R, Ghosh A, Ledwich G, Zare F. Load sharing and power quality enhanced operation of a distributed micro-grid. IET Renewable Power Generation. 2009;**3**(2):109-119

[13] Nayar C. Innovative remote microgrid systems. International Journal of Environment and Sustainability. 2012;**1**(3):53-65

[14] Kawasaki K, Matsumura S, Iwabu K, Fujimuram N, Iima T. Autonomous dispersed control system for independent microgrid. Journal of Electrical Engineering, Japan. 2009; **166**(1):1121-1127

[15] Li X, Song Y, Han S. Frequency control in microgrid power system combined with electrolyzer system and fuzzy PI controller. Journal of Power Sources. 2008;**180**:468-475

[16] Basu AK, Chaowdhury SP, Chaowdhury S, Ray D, Crossley PA. Reliability study of a microgrid system. IEEE Transactions on Power Systems. 2006;**21**(4):1821-1831

[17] Karki R, Hu P, Billinton R. Reliability evaluation considering wind

and hydropower coordination. IEEE Transactions on Power Systems. 2010; **25**(2):685-603

[18] Tanrioven M. Reliability and cost-benefits of adding alternate power sources to an independent micro-grid community. Journal of Power Sources. 2005;**150**:136-149

[19] Zhou P, Jin RY, Fan LW. Reliability and economic evaluation of power system with renewables: A review. Renewable and Sustainable Energy Reviews. 2016;**58**:537-547

[20] Acuna L, Padilla RV, Mercado AS. Measuring reliability of hybrid photovoltaic-wind energy systems: A new indicator. Renewable Energy. 2017; **106**:68-77

[21] Adefarati T, Bansal RC. Reliability assessment of distribution system with the integration of renewable distributed generation. Applied Energy. 2017;**185**: 158-171

[22] Li J, Wei W. Probabilistic evaluation of available power of a renewable generation system consisting of wind turbine and storage batteries: A Markov chain method. Journal of Renewable and Sustainable Energy. 2014;**6**(1): 1493-1501

[23] Liu X, Chowdhury AA, Koval DO. Reliability evaluation of a wind-diesel-battery hybrid power system. In: IEEE Industrial and Commercial Power Systems Technical Conference; 2008

[24] Wang L, Singh C. Adequacy assessment of power-generating systems including wind power integration based on ant colony system algorithm. In: IEEE Lausanne Power Tech; 2007

[25] Wen J, Zheng Y, Donghan F. A review on reliability assessment for wind power. Renewable and Sustainable Energy Reviews. 2009;**13**:2485-2494

[26] Bhuiyan FA, Yazdani A. Reliability assessment of a wind power system with integrated energy storage. IET Renewable Power Generation. 2010;**4**(3):211-220

[27] Choi J, Park JM, Shahidehpour M. Probabilistic reliability evaluation of composite power systems including wind turbine generators. In: Proc. of IEEE International Conference on Probabilistic Method Applied to Power Systems; 2010. pp. 802-807

[28] Vallee F, Lobry J, Deblecker O. System reliability assessment method for wind power integration. IEEE Transactions on Power Systems. 2008; **23**(3):1288-1297

[29] Silva AMLD, Manso LAF. Application of Monte-Carlo simulation to generating system well-being analysis considering renewable sources. European Transactions on Electrical Power. 2007;**17**:387-400

[30] Arifujjaman M. Performance and reliability comparison of grid connected small wind turbine systems. PhD dissertation. NL, CA: Department of Electrical and Computer Engineering, Memorial University of Newfoundland, St. John's; 2010

[31] Ebeling CE. An Introduction to Reliability and Maintainability Engineering. USA: Waveland Press; 2010

[32] Vittal S, Teboul M. Performance and reliability analysis of wind turbines using Monte-Carlo methods based on System Transport Theory. In: Proc. of Structural Dynamics and Materials Conference; 2005. pp. 1-8

[33] Oettinger FF, Blackburn DL, Rubin S. Thermal characteristics of power transistors. IEEE Transactions on Reliability. 1976;**23**(8):831-838

[34] Ali MH. Wind Energy Systems: Solutions for Power Quality and Stabilization. USA: CRC Press; 2012

[35] Feix G, Dieckerhoff S, Allmeling J, Schonberger J. Simple methods to calculate IGBT and diode conduction and switching losses. In: Proc. of 13th European Conference on Power Electronics and Applications; 2009. 8-10

[36] Bierhoff MH, Fuchs FW. Semiconductor losses in voltage source and current source IGBT converters based on analytical derivation. In: Proc. of IEEE Power Electrics Specialist Conference; 2004. pp. 2836-2842

[37] Mestha LK, Evans PD. Analysis of on-state losses in PWM inverter. IEE Proceedings. 1989;**136**(4):1989

IntechOpen